Crack propagation across an adhesive interlayer in flexural loading

James Jin-Wu Lee,[a] Herzl Chai,[b] Isabel K. Lloyd[a] and Brian R. Lawn[c,*]

[a]*Department of Materials Science and Engineering, University of Maryland, College Park, MD 20742-2115, USA*
[b]*School of Mechanical Engineering, Tel Aviv University, Tel Aviv, Israel*
[c]*Materials Science and Engineering Laboratory, National Institute of Standards and Technology, Gaithersburg, MD 20899-8500, USA*

Crack propagation across interlayers separating adjoining brittle plates in flexure was studied using a model glass/epoxy/glass system. A transverse starter crack in the center glass plate was made to propagate to the nearest epoxy interface, where it arrested. System failure occurred at some higher load by crack reinitiation from pre-existing flaws in the adjoining glass surface, not by continuous penetration through the epoxy. A fracture mechanics analysis was developed to elucidate the role of material and geometrical variables.
Published by Elsevier Ltd. on behalf of Acta Materialia Inc.

Lamination is an effective route to improving damage tolerance and energy absorption of otherwise brittle materials. The special case of a crack intersecting a bilayer interface has received considerable attention [1–3]. The crack may arrest, deflect and delaminate, or penetrate into the adjacent layer. In the case of a trilayer consisting of two brittle plates with an intervening compliant or soft interlayer, the crack may reinitiate discontinuously within the second brittle layer [4] or penetrate continuously through the adhesive into the second brittle layer. The fracture behavior in such systems depends on the geometric and material properties of the constituents, the quality of the interface and the mode of loading. The adhesive may be considered to "shield" the adjoining brittle layers from the field of the approaching crack, thus providing a means of crack containment. This concept of containment is implicit in a wide variety of engineering applications, including laminated window glasses and car windshields [5], biological shell structures [6,7], and teeth and dental crowns [8].

Here we devise a simple model glass/epoxy/glass system to quantify the role of adhesive interlayers in crack containment. In a companion work, we studied this role by driving cracks to the interface using a line-wedge indenter [9]. While usefully demonstrating the effective shielding role of compliant interlayers, that specific test configuration was limited by chipping problems

at the upper line contact, exacerbated by an exceptionally high shielding of applied stresses in the lower brittle plate by the adhesive interlayer, making it difficult to investigate crack reinitiation across thicker interlayers. The alternative configuration shown in Figure 1 overcomes this difficulty. Glass plates of modulus $E_1 = 70$ GPa are bonded with epoxy of modulus $E_2 = 2.8$ GPa. The center and outer glass plates have widths $2w = 1$ mm and $W = 2.2$ mm, respectively, and common thickness (normal to plane of diagram) $d = 5.5$ mm. The adhesive thickness varies between $h = 1$ μm and 1 mm. The surfaces of the center glass plate are joined in their as-polished state, but the opposing surfaces of the outer plates are either pre-abraded with SiC grit to introduce a controlled population of flaws (low-strength state) or pre-etched to remove them (high-strength state) [9]. A starter crack of length $2c \approx 190$ μm is introduced at the center of the inner glass plate using a Vickers indentation at load 10 N. The system is then loaded in flexure, span dimensions $a = 10$ mm and $b = 40$ mm, placing the top surface of the specimen in tension and propagating the crack toward the nearest glass/epoxy interface. In the approximation of small pre-failure crack dimensions (i.e. $w \ll W$, $w \ll b$), the maximum transverse strain across the specimen section may be determined from the breaking force P using the routine strength-of-materials relation $\varepsilon = (3Pa/4E_1wd^2)/(1 + E_2h/E_1w + W/w)$. The tensile stresses in the glass and adhesive layers are $\sigma_1 = E_1\varepsilon$ and $\sigma_2 = E_2\varepsilon$. A video camera is used to follow in real time the progress of the crack as it intersects the

* Corresponding author. E-mail: brian.lawn@nist.gov
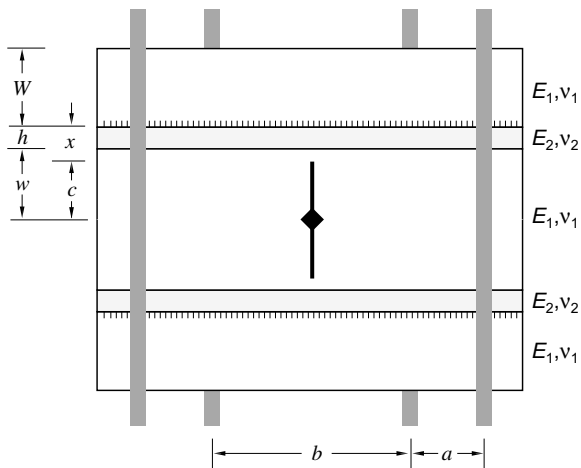
Figure 1. Schematic of glass/epoxy/glass trilayer in four-point flexural loading. Vickers indentation used to introduce a starter crack at the top center of the inner glass plate. Inner surfaces of the outer glass plates are abraded, to introduce a uniform density of surface flaws, or etched, to eliminate flaws.

interface and, at some load increment, finally traverses the adhesive and fractures the adjacent layers. The aim is to confirm the dominance of a reinitiation mode of failure, and to quantify the critical values of tensile strain ε to achieve such failure in terms of geometrical and material parameters.

Typical crack evolution data are plotted in Figure 2, as applied strain ε vs. crack size c, for adhesive thickness $h = 100\ \mu m$. The experimental observations are shown as horizontal bands, with arrows indicating stages of unstable crack propagation—the bands represent standard deviation scatter bounds in strain data (minimum 10 tests). The curves are theoretical predictions of $\varepsilon(c)$ (see below). Load is increased steadily until the Vickers crack becomes unstable at a mean strain of $\varepsilon \approx 0.52 \times 10^{-3}$ and arrests at the first interface. This initial phase of the evolution is independent of the flaw state in the adjoining glass plates, as expected. With fur-

ther increase in strain the crack abruptly appears in the adjoining glass plates and takes the system to immediate failure. (The optics lacked the necessary resolution to determine the extent of any crack penetration into the thin adhesive interlayer during this phase of loading.) The critical strain required to achieve this failure is now highly dependent on the flaw state in the outer plates: in the case of abraded surfaces the mean critical strain is $\varepsilon \approx 0.95 \times 10^{-3}$, amounting to a factor of ~2 increase over the arrest strain; in the case of etched surfaces the critical strain is much higher, $\varepsilon \approx 2.5 \times 10^{-3}$, i.e. a factor of ~5 increase. Since continuous crack penetration through the adhesive would be independent of glass flaw state, this is clear evidence in favor of the reinitiation mode of failure. Another clue is obtained from examination of broken specimens: with abraded surfaces (Fig. 3a) the reinitiated cracks appear nearly collinear with the primary crack, indicating the inevitable presence of a suitable flaw in the outer glass plate immediately ahead of the crack tip; with etched surfaces (Fig. 3b) the crack path is substantially dislocated across the interlayer, as if the stress field of the primary crack had to "search" for the occasional flaw in the outer glass plate.

Of principal interest in the context of crack-containment capacity is the effect of interlayer thickness h on the critical reinitiation strain ε_I. Figure 4 shows data for ε_I over a broad range of h, for outer glass layers with abraded surfaces. The lines are predictions (below). As intuitively expected, $\varepsilon_I(h)$ is a monotonically increasing
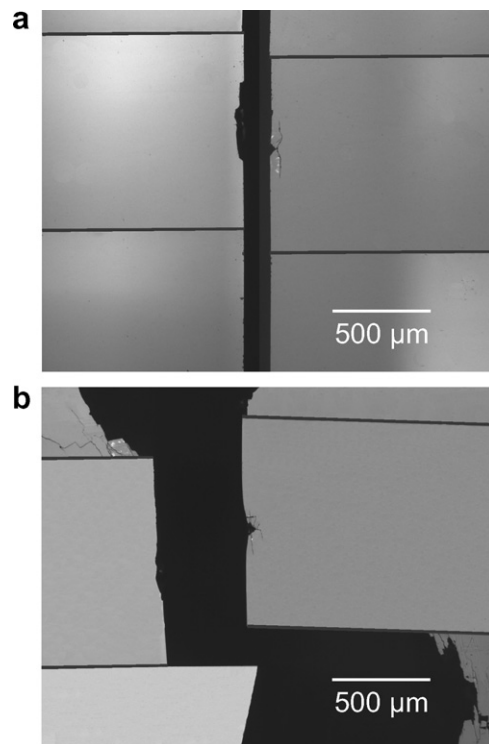
Figure 3. Post-fracture micrographs for glass plates with epoxy interlayer, $h = 10\ \mu m$, with (a) abraded and (b) etched adjoining glass surface. Vickers indentations visible at center. Note near-collinear crack in (a), disjointed crack in (b).

Figure 2. Applied tensile strain ε as function of crack length c for glass/epoxy/glass configuration with Vickers starter cracks. Data for specimens with abraded (A) or etched (E) surfaces, for $h = 100\ \mu m$. Arrows indicate unstable crack extension, bands indicate standard deviation bounds. Curves are plots of functions $\varepsilon_P(c)$ from Eq. (3) and $\varepsilon_I(c)$ from Eq. (5).
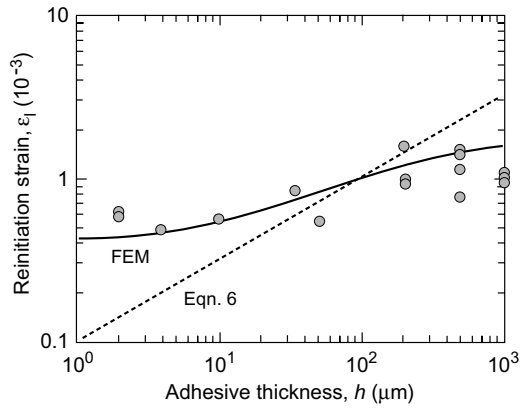
Figure 4. Critical strain ε_I for crack reinitiation vs. interlayer thickness h for glass/epoxy/glass trilayers. Dashed curve corresponds to simplified failure stress condition in Eq. (6); solid curve is FEM calculation.

function, although the observed rate of increase is not strong.

It is instructive to analyze the data in Figures 2 and 4 in terms of fracture mechanics. We do this by comparing crack reinitiation in the adjacent brittle layer ahead of the arrested crack tip with continuous crack penetration through the adhesive. Consider crack penetration first. The stress intensity factor for a crack in a monolith of modulus E_1 has the form

$$K_0 = \varepsilon E_1 (\pi c)^{1/2}. \tag{1}$$

For a system with adhesive interlayer we may write

$$K = \Phi K_0, \tag{2}$$

where $\Phi = \Phi(c/w, h/w, E_2/E_1, v_2/v_1)$ is a dimensionless correction function defining the influence of the interlayer, and v is Poisson's ratio. Whether the crack will extend in any given layer is then determined by the condition $K = T = K_{IC}$, where T is the toughness of the layer containing the crack tip. Eqs. (1) and (2) may then be combined to obtain a normalized strain relation for equilibrium crack penetration

$$\varepsilon_P = [T/E_1(\pi w)^{1/2}][(w/c)^{1/2}/\Phi(c/w)] \tag{3}$$

for any given E_2/E_1 and h/w. The strain ε_P is plotted in normalized form as a function of c/w in Figure 5a corresponding to our experiments, with $\Phi = \Phi(c/w)$ computed from finite element modeling (FEM) and inserting $h/w = 100\,\mu m/500\,\mu m = 0.20$, $E_2/E_1 = 2.8$ GPa/70 GPa $= 0.040$ and $v_2/v_1 = 0.35/0.25 = 1.4$, and assuming $T = T_1 = T_2$ (to emphasize the modulus mismatch effect) [9]. The inclined dashed line corresponds to the condition $\Phi = 1$ for a monolithic brittle solid. The degree of departure of ε_P from this dashed line quantifies the shielding effect of the compliant interlayer. This plot shows that a penetrating crack is increasingly attracted to the interface while in the first brittle layer, but is then increasingly repulsed by the adjoining brittle layer while in the interlayer.

Now consider crack reinitiation from the inner surface of one of the adjoining glass plates in the field of the primary crack arrested either at the first glass/epoxy interface or within the epoxy itself. The usual condition
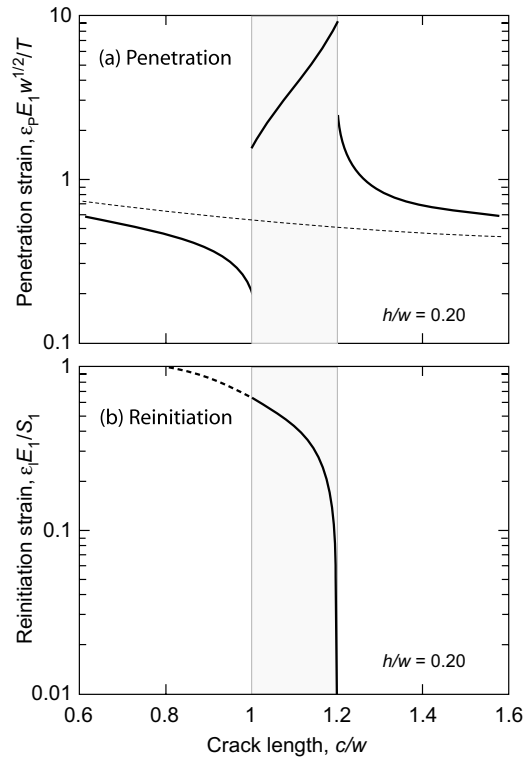
Figure 5. Normalized plots of penetration function $\varepsilon_P(c)$ from Eq. (3) and reinitiation function $\varepsilon_I(c)$ from Eq. (5), for $T = T_1 = T_2$.

for such a failure is that the maximum tensile stress at the adjoining glass surface just equals the strength $S_1 = T_1/(\pi c_f)^{1/2}$, where c_f is a characteristic flaw size [4,9]. This maximum stress can be approximated by [4]

$$\sigma = K_0/(2\pi x)^{1/2} \tag{4}$$

within the region $x \ll c$, where $x = w + h - c$ in Figure 1. Inserting $\sigma = S_1$ into Eqs. (1) and (4) then yields a reinitiation strain

$$\varepsilon_I = (S_1/E_1)[2(w/c + h/c - 1)]^{1/2} \tag{5}$$

The function $\varepsilon_I(c/w)$ is plotted in normalized form in Figure 5b, for the same h/w as in Figure 2. This function decreases monotonically up to $c = w + h$, i.e. for cracks propagating within either the first glass layer or the adhesive. A special case of Eq. (5) is for primary cracks that reinitiate after arrest at the first interface. Inserting $c = w$ into Eq. (5) yields

$$\varepsilon_I = (S_1/E_1)(2 h/w)^{1/2} \tag{6}$$

This relation emphasizes the role of interlayer thickness h in the reinitiation process.

Casual inspection of Figure 5a and b indicates that the $\varepsilon_I(c/w)$ and $\varepsilon_P(c/w)$ curves must intersect just within the adhesive interlayer, signaling an abrupt transition to reinitiation from penetration shortly after arrest. Exactly where this transition takes place will depend on the values of the material parameters E_1, S_1 and T_1 in Eqs. (3) and (5). We include predictions from these equations in Figure 2, using the following values: $E_1 = 70$ GPa, $E_2 = 2.8$ GPa, $T_1 = 0.6$ MPa m$^{1/2}$, $T_2 = 1$ MPa m$^{1/2}$, $S_1 = 115$ MPa (abraded glass),

$S_1 = 300$ MPa (etched glass) [9]. The intersection locations between $\varepsilon_I(c/w)$ and $\varepsilon_P(c/w)$ curves correspond to the configurations where reinitiation takes place in the outer glass layer. Note in particular how this intersection point shifts upward for etched relative to abraded glass surfaces. While not accurately indicative of absolute values, this shift nevertheless mirrors that of the corresponding failure strains in the experimental data, providing quantitative validation for the reinitiation mode.

Predictions of critical reinitiation strain are also included in the $\varepsilon_I(h)$ diagram of Figure 4. The dashed line is a plot of Eq. (6), assuming the primary crack to be arrested at the first interface and inserting $S_1 = 115$ MPa for abraded glass. While accounting for a monotonically increasing $\varepsilon_I(h)$, this approximation does not represent the data well. As in the preceding companion paper [9], we examine the trends more closely in a refined calculation by FEM, taking into account the effect of stress gradients in the crack-tip field over the length of abrasion flaws of length $c_f = 18$ μm in the outer glass layer. Briefly, the analysis determines the stress intensity factor at the tip of the flaw using the Irwin crack-opening displacement approach [9]. These gradients account for the higher strains needed to reinitiate cracks across ultra-thin interlayers in Figure 4 (left). The data show that even the thinnest adhesive bonds can be effective as crack arrestors. The FEM analysis also incorporates the effect of flexural stresses in the adjoining glass layers, superposed onto the crack-field stresses in Eq. (4) (neglected in our formulation of Eqs. (5) and (6)). In this case, the calculation accounts for the plateau in the $\varepsilon_I(h)$ data for thick interlayers in Figure 4 (right).

This work confirms that compliant interlayers are highly effective as agents of crack containment. Such containment arises primarily from shielding of adjacent brittle layers from the field of an advancing primary crack, rather than from enhanced toughness. The degree of shielding is dependent on the mode of loading. In the present case the flexural loading generates a more or less uniform state of strain at the specimen top surface, so that a crack may more easily jump from layer to layer than with a specimen with line- or point-force loading, especially for thicker layers. Reinitiation remains the dominant mode of crack spreading, at least for the compliant epoxy adhesive used here. A stiffer interlayer will inevitably reduce the shielding [9], until ultimately, as the modulus of the adhesive approaches that of the brittle layers, continuous penetration becomes ever more possible. On the other hand, stiffer interlayers may suppress subsidiary fracture modes, such as radial fracture from the surface of a flexing center plate in surface-contact loading [10]. Designing for ultimate fracture resistance and crack containment clearly calls for compromises, with due attention to loading configuration as well as to interlayer dimensions and material properties.

[1] M.-Y. He, J.W. Hutchinson, Int. J. Solids Struct. 25 (1989) 1053.
[2] W.J. Clegg, K. Kendall, N.M. Alford, T.W. Button, J.D. Birchall, Nature 347 (1991) 455.
[3] T. Fett, D. Munz, Stress Intensity Factors and Weight Functions, Computational Mechanics Publications, Southampton, 1997.
[4] M.C. Shaw, D.B. Marshall, M.S. Dadkhah, A.G. Evans, Acta Metall. 41 (1993) 3311.
[5] P.V. Grant, W.J. Cantwell, H. McKenzie, P. Corkhill, Int. J. Impact Eng. 21 (1998) 737.
[6] J.D. Currey, Proc. Roy. Soc. Lond. 196 (1977) 443.
[7] S. Kamat, X. Su, R. Ballarini, A.H. Heuer, Nature 405 (2000) 1036.
[8] B.R. Lawn, S. Bhowmick, M.B. Bush, T. Qasim, E.D. Rekow, Y. Zhang, J. Am. Ceram. Soc. 90 (2007) 1671.
[9] J.J.-W. Lee, I.K. Lloyd, H. Chai, J.-G. Jung, B.R. Lawn, Acta Mater., in press.
[10] J.J.-W. Lee, Y. Wang, I.K. Lloyd, B.R. Lawn, J. Dent. Res. 86 (2007) 745.